Journal of Materials Chemistry C

Accepted Manuscript

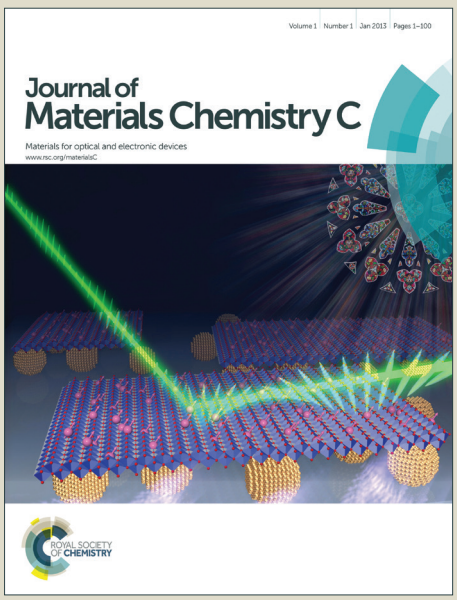

ROYAL SOCIETY OF CHEMISTRY

www.rsc.org/materialsC

Growing gold nanoparticles on a flexible substrate to enable simple mechanical control of their plasmonic coupling

Ugo Cataldi,[a,b] *Roberto Caputo,*[b] *Yuriy Kurylyak,*[b] *Gérard Klein,*[a] *Mahshid Chekini,*[a] *Cesare Umeton,*[b] *Thomas Bürgi**[a]

[a] Department of Physical Chemistry, University of Geneva, 30 Quai Ernest-Ansermet, 1211 Geneva 4, Switzerland

e-mail: thomas.buergi@unige.ch

[b] Department of Physics, Centre of Excellence for the Study of Innovative Functional Materials CEMIF-CAL, University of Calabria and LICRYL - IPCF (Liquid Crystals Laboratory, Institute for Chemical Physics Processes) CNR – UOS Cosenza, 87036 Arcavacata di Rende, Italy

Abstract

A simple method is presented to control and trigger the coupling between plasmonic particles using both a growing process of gold nanoparticles (GNPs) and a mechanical strain applied to the elastomeric template where these GNPs are anchored. The large scale samples are prepared by first depositing and then further growing gold nanoparticles on a flexible PDMS tape. Upon stretching the tape the particles move further apart in the direction of the stretching and closer together in the direction perpendicular to it. The synergy between the controlled growth of GNPs and the mechanical strain, leads to a drastic shift of the plasmon band and a color change of the sample. Furthermore, the stretching by only a few percent of the amorphous and initially isotropic sample results in a strong polarization-dependent plasmon shift. At smaller gap sizes between neighboring particles, induced by stretching the PDMS tape, the plasmon shift strongly deviates from the behaviour expected considering the plasmon ruler equation. This shows that multipolar coupling effects significantly contribute to the observed shift. Overall, these results indicate that a macroscopic mechanical strain allows one to control the coupling and therefore the electromagnetic field at the nanoscale.

Introduction

Metal nanoparticles show characteristic colours when illuminated by light due to their plasmon resonances.[1-3] In addition, when nanoparticles are very close to each other, near-field coupling leads to concentrated and highly localized electric fields.[4, 5] This phenomenon is at the origin of many applications in sensing,[6-9] in the design of metamaterials,[10, 11] for single molecule

detection,[12, 13] and in spectroscopic techniques.[14] The coupling and optical properties of a sample sensitively depend on the distance between nanoparticles.[15, 16] In particular, in the prototypical example of a gold nanoparticle dimer, the coupling leads to a shift of the plasmon resonance in the extinction spectrum once the gap between the two particles is as small as half of their diameter or less.[17] Since this shift depends exponentially on the gap between the coupled particles,[18, 19] interesting opportunities emerge from the possibility to dynamically control, at the nanometer scale, the distance between the coupled plasmonic particles of a macroscopic sample.[20-24]

Here we show that realization of this control is as simple as pulling an elastic tape covered by gold nanoparticles. The distance between them is controlled by growing the deposited nanoparticles and by mechanically stretching the elastic tape in one direction, which leads to a compression in the direction perpendicular to the stretching one. The result is a reversible colour change of the sample. At the nanoscale, this means that the electric interaction between the particles can be manipulated by using a reversible mechanical strain. The precise control of the nanogaps between neighbouring nanoparticles, obtained by means of the growth process, is fundamental for achieving the mechanical control over the optical properties of the sample.

Results and discussion

The basic idea is given in Fig. 1a, whereas the real system is shown in Fig. 1b,c: upon stretching, the colour changes from magenta to blue-violet. Samples have been prepared by using self-assembly techniques from nanochemistry (see experimental part for details). The fabrication process is resumed in Scheme 1.

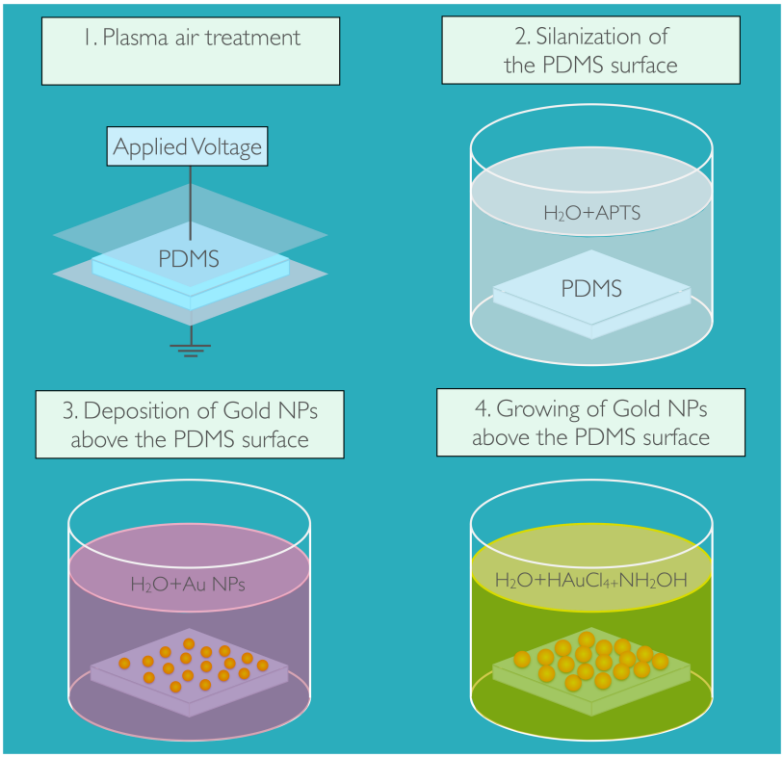

Scheme 1. Sketch of the process followed for fabricating samples made of PDMS substrates with a monolayer of grown gold NPs immobilized on the surface.

We first functionalized a flexible polydimethylsiloxane (PDMS) substrate by silanization chemistry using 3-aminopropyltriethoxysilane (Scheme 1, step 1,2). This imparts a positive charge to the PDMS surface so that gold nanoparticles spontaneously adsorb in a charge-driven process (Scheme 1, step 3). The resulting surface (Fig. 2a) reveals an amorphous arrangement of well-separated non-interacting particles (average diameter 23 nm) with an average nearest neighbour distance (centre-to-centre) of 39 nm. We then grew the gold nanoparticles in size, which was done by dipping the sample in a Au^{3+}/NH_2OH solution at room temperature for 2 min (Scheme 1, step 4). Under these conditions the Au^{3+} ions are reduced at the surface of the gold nanoparticles (but not in solution) thus increasing their diameter (D) and decreasing the gap (s)

between them, to a point where coupling effects start to become relevant. In the sample shown in Fig. 2b, the grown nanoparticles have an average diameter of about 32 nm. At this stage, the simple stretching (of a few percent) of the tape in one direction, which leads to a compression in the orthogonal one, is used to induce strong variations in the coupling between particles. In literature, other ways are reported to obtain plasmon tunability and/or coupling between nanoparticles of fixed size, coated on, or embedded in, flexible substrates.[20-24] What distinguishes our work from previous ones is the growth process. In fact, the fine increase of particle size is a fundamental condition to obtain coupling: the growth gradually reduces the inter-particle gap up to the trigger of the plasmon coupling, whereas the application of a mechanical stretching allows its reversible tuning. Macroscopically, this is evidenced by a colour change of the sample and a polarization dependent change of the extinction spectra (Figs 2c,d); in fact, the latter reveal a shift of the plasmon resonance (when stretching the tape) that is at the origin of the colour change. According to the plasmon ruler equation,[18] the relative shift ($\Delta\lambda/\lambda_0$) of the plasmon band, calculated as the ratio between the absolute plasmonic shift $\Delta\lambda$ and the single-particle resonance peak maximum wavelength λ_0 (measured on the sample at rest and before growing the particles), exponentially depends on *s/D*:

$$\frac{D\lambda}{\lambda_0} = k\exp\left(-\frac{s}{\tau D}\right) \quad (1)$$

where *s* is the gap between particles of diameter *D*, while *k* is the maximum plasmonic shift for the particle dimer and τ is a decay constant that depends on the considered system. PDMS has a Poisson ratio of about 0.5,[25] which has been verified also for our sample (Supplementary Information, Fig. S1); thus stretching the sample 20% in one direction, leads to a compression of 10% in the orthogonal direction. Using the experimental parameters for particle

size and separation, we can estimate the following: Particles of 32 nm diameter (after growth) and a center-to-center distance of 39 nm are separated by a gap of 7 nm. Reducing the separation by 3.9 nm (reduction by 10% of center-to-center distance due to compression) reduces the gap to 3.1 nm or by 56%. This is an effect that, due to the exponential dependence of the plasmon shift on *s*, turns out to be dramatic.

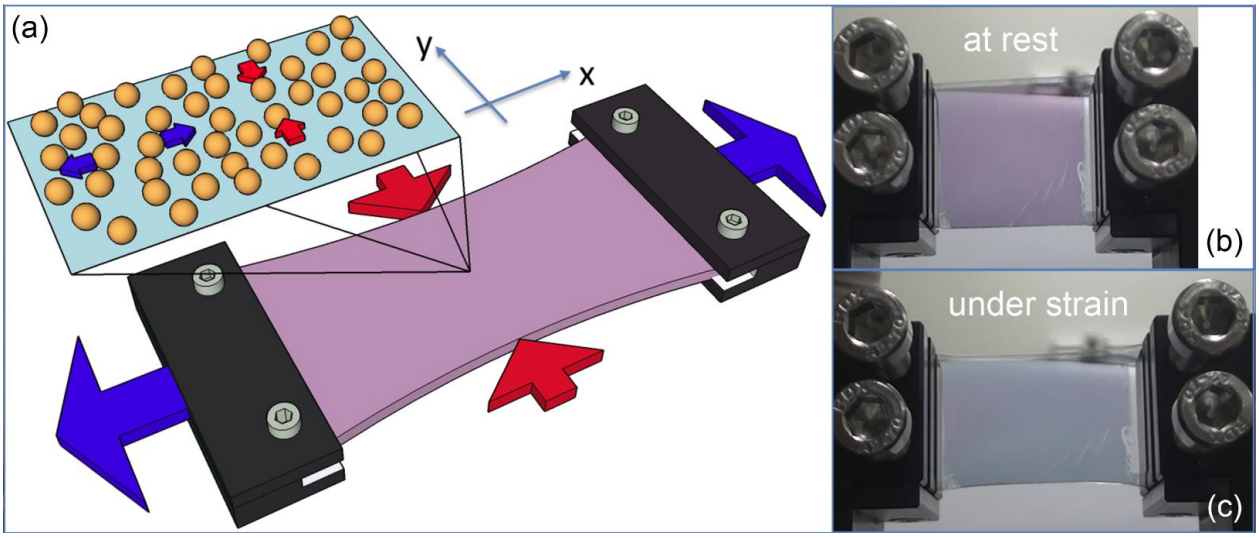

Fig. 1 (a) Sketch of the experimental setup. By stretching a PDMS sample coated with a single layer of gold nanoparticles the average distance between them becomes larger in the stretching direction and shorter in the perpendicular one. Stretching of the sample is accompanied by a remarkable change of colour from purple-red (b) to blue-violet (c). Images were acquired with a polarizer, mounted to a camera, with direction of polarization perpendicular to the applied strain.

Important parameters which determine the performance of the sample are the initial density of nanoparticles (2046 particles/μm^2, as determined from SEM images), which defines the average nearest neighbour separation, and the number of growth cycles (two minutes each), which affects the particle size. In Figs. 2a,b, SEM micrographs of the sample before and after undergoing twelve growth cycles are shown, while Figs. 2c,d report the extinction spectra of the latter

sample for different stretching percentage values. The plasmon band, acquired after growing the nanoparticles and with the sample at rest, is broadened and slightly red-shifted with respect to the one of perfectly spherical and isolated gold nanoparticles. This could be due to weak coupling between particles and/or the deviation from perfect spherical shape after growing. However, the SEM image after growing (Fig. 2b) does not indicate a large deviation from the spherical shape. Spectra have been acquired by irradiating the sample with ⊥-polarized light (with respect to stretching direction), first by increasing (Fig. 2c) and then by releasing the applied strain (Fig. 2d). The behaviour observed in Figs. 2c,d is almost the same, denoting that the changes induced in the sample are fully reversible (see also the video in the supplementary information). In Fig. S1 (Supplementary Information), the measurement of the percentage compression that the sample undergoes in the direction perpendicular to the applied strain is reported; a Poisson coefficient of about 0.5 is confirmed, which indicates that the sample remains in the elastic regime for all the applied strains. Fig. S2 (Supplementary Information), reports the spectral position of the resonance peak maxima as a function of the strain during a straining-releasing cycle. The optical properties are reversible.

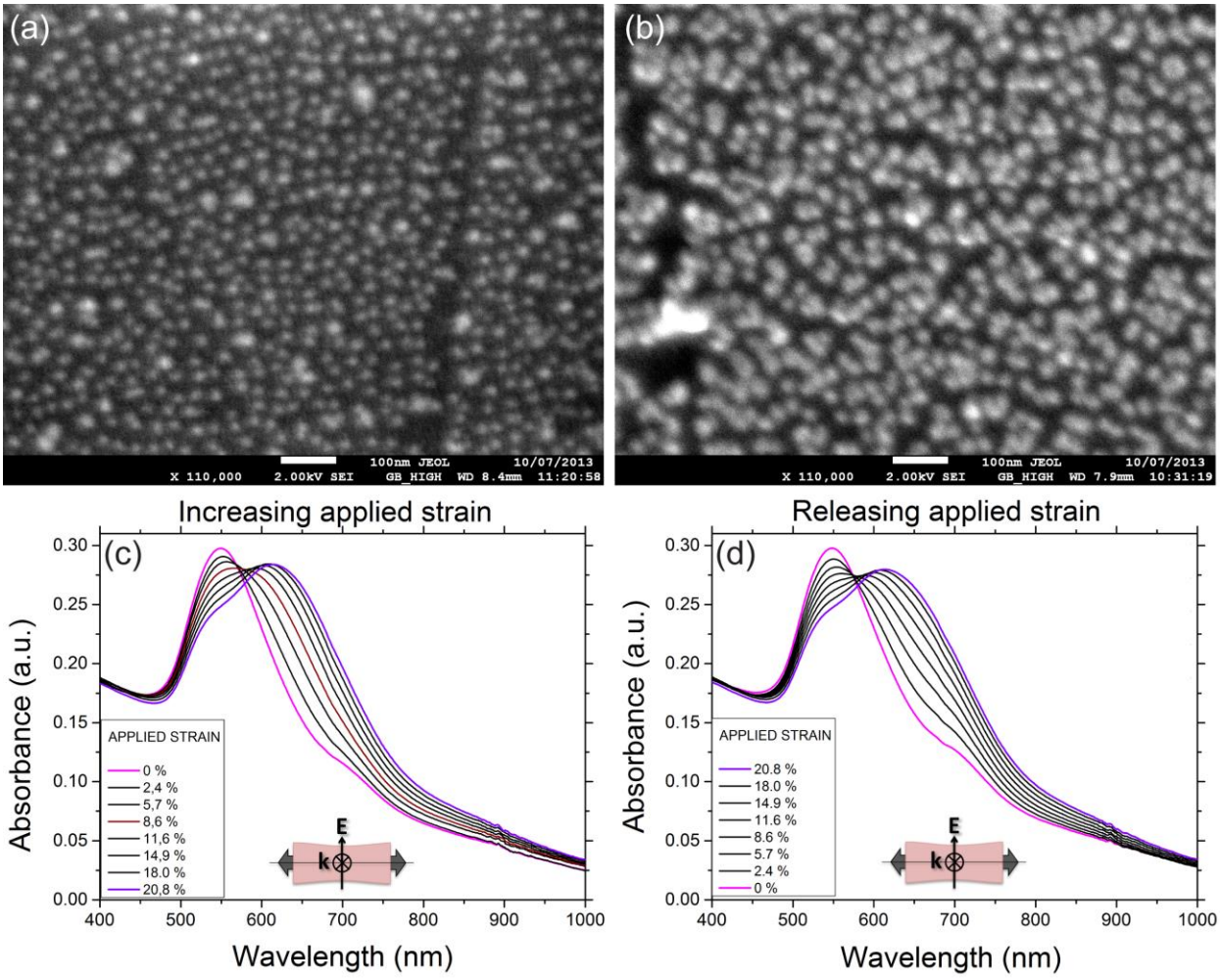

Fig. 2 SEM micrographs of a gold nanoparticle coated PDMS substrate, taken (a) before and (b) after twelve growth cycles; (c) Extinction spectra of the sample coated with gold nanoparticles (after twelve cycles of growth) acquired while increasing the applied strain from 0% to 20.8%. The sample was irradiated with ⊥-polarized light (**E** field perpendicular to the stretching direction). (d) Extinction spectra acquired by releasing the strain applied to the same sample from 20.8% to 0%..

The most striking feature emerging from curves shown in Figs 2c,d is a change of shape of the plasmon resonance extinction band due to a simple stretching of the sample. At the maximum elongation (20.8%), Fig. 2c clearly shows the presence of two peaks in the absorbance curves. During the stretching experiment, the amplitude of the original dipolar peak (due to perfectly

spherical and isolated gold nanoparticles) decreases and, at the same time, the show-up and increase of a second red-shifted peak is observed. While increasing the applied strain, the spectral position of the maximum of this second peak is continuously red-shifted. This behaviour suggests that, during the stretching of the sample, two populations of nanoparticles emerge. Namely, the first population (corresponding to the dipolar peak) is related to non-interacting particles and decreases with increasing strain; the other one is due to particles undergoing a plasmon coupling (red-shifted peak), which increases with strain. In the Supplementary Information, a qualitative explanation of this hypothesis is provided, while further studies are already in progress to quantitatively demonstrate it.

In order to get a better insight into the plasmonic behaviour of the system and to identify those conditions (particle size and/or average gap between them) that can prove critical for the coupling of particles, extinction spectra of the sample, at rest and under stress, have been acquired after each growth cycle. Fig. 3a shows spectra measured at the maximum elongation (20.8%) as a function of the number of growth cycles, while corresponding spectra of the same samples, at rest, are shown in Fig. 3b. Spectral positions of the maxima of the extinction band are also reported for the same samples, both at rest and stretched (Fig. S3 in Supplementary Information).

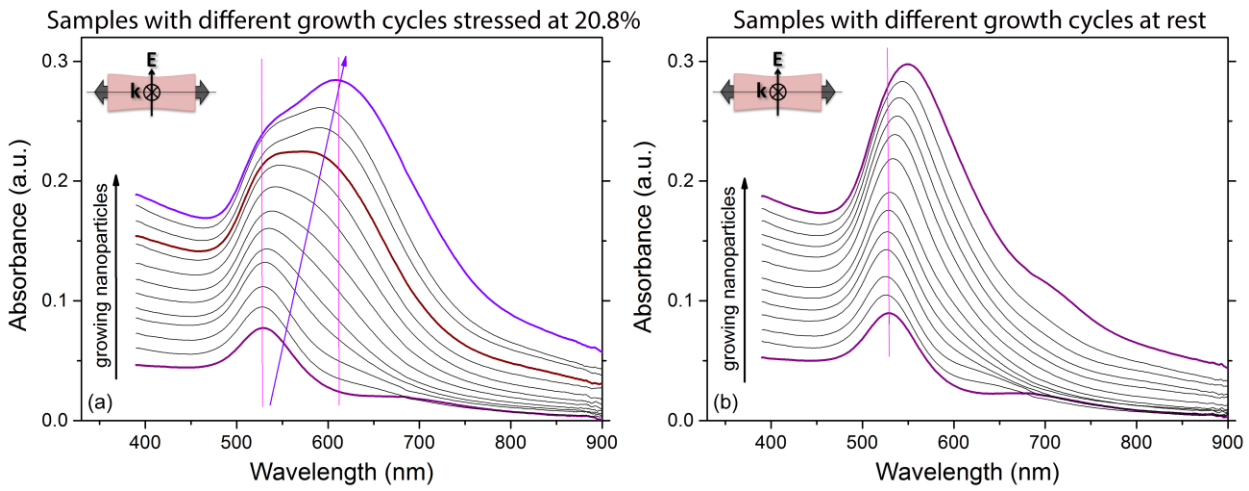

Fig. 3 Extinction spectra of gold nanoparticle coated PDMS samples with different numbers of growth cycles of particles, in case that (a) an applied strain of 20.8% is applied and (b) samples are at rest. Samples are irradiated with ⊥-polarized light (**E** field perpendicular to the stretching direction).

In samples at rest, the growth of particles leads to a moderate shift of the localized surface plasmon resonance (triangles in Fig. S3 in Supplementary Information). When a strain is applied (stars in Fig. S3 in Supplementary Information) and after few growth cycles (three to eight), a moderate though larger shift is observed. Noteworthy, after many cycles (nine to twelve) the stretching has a dramatic effect: in fact, particles in the relaxed state are so close that a slight change in their relative distance has a huge impact on the coupling effect and hence on the resonance shift.

Our samples, which are amorphous and initially isotropic in the *x*-*y* plane, develop significant polarization-dependent optical properties after undergoing a stretching of about 20% only. A way to interpret this behaviour is to consider the interaction energy of a dimer. The polarized illumination induces a dipole in each nanoparticle; the dimer can be represented, therefore, by two parallel dipoles, initially separated by a distance vector ***r*** (center-to-center)**,** which forms an

angle α with the stretching direction (x). Thus, the coupling between nanoparticles can be qualitatively described in the framework of the exciton-coupling model[26], originally developed to explain shifts observed in the spectra of dimerized organic molecules. The interaction energy U between the two particles of a dimer changes upon stretching and it is a function of the angle α. The energy variation ΔU between two differently stretched states can be both positive or negative, corresponding to a blue or a red-shift of the plasmon band, respectively, as demonstrated in the past.[17] Application of such a model qualitatively reproduces the shifts observed during stretching (a detailed description is given in the Supplementary Information).

For a more quantitative description of the phenomenon, it is convenient to evaluate the plasmonic shift normalized to the single-particle resonance wavelength ($\Delta\lambda/\lambda_0$) as a function of the normalized gap (s'/D) between nanoparticles. To enable this calculation, a k-neighbours algorithm has been implemented, which exploits the SEM micrographs of samples before and after growing the particles (Figs. 2a,b). The code enables identification of the particle centers (Fig. S4 in Supplementary Information) and calculates the distance r (center-to-center) between each particle and its nearest neighbours (see experimental section). In Fig. 4, the experimental dependence of $\Delta\lambda/\lambda_0$ on s'/D (normalized plasmon shift and normalized interparticle gap respectively of the samples under stretching) is plotted for samples with a different number of cycles of growth (from seven to twelve cycles). Each absorption spectrum has been acquired several times by changing, each time, the value of the applied mechanical stress δ (0%; 2.4%; 5.6%; 8.6%; 11.6%; 14.9%; 18.0%; 20.8%). In this graph, only curves related to samples with more than seven growing cycles have been included. This is due to the fact that only these samples satisfy the condition (size of nanoparticles and mechanical strain) enabling the triggering of the plasmon coupling. In general feature, when the coupling is triggered, a drastic

shift of the plasmon resonance takes place and the overall experimental behaviour can be fitted with an exponential function (equation (1)). This condition is also verified in our case. As an example, the fit of the curve related to the sample with ten cycles of growth (solid black curve in Fig. 4) is exponential and yields parameters: k = 2.7±0.4 and τ = 0.029±0.001. However, the same curve does not completely fit the other experimental results reported in Fig. 4. Indeed, taking a closer look at Fig. 4 (and its inset) it can be noticed that the agreement of the fitting curve with the experimental ones depends on the considered range of s'/D values. For 0.15<s/D<0.25, the different samples, independently of their nanoparticle sizes, follow the same exponential function as predicted by the plasmon ruler equation (see inset of Fig. 4). On another hand, for s'/D<0.15, the size-scaling, mainly related to the dipolar coupling picture[17], disappears and the behavior becomes slightly dependent on particle size. In case s'/D<0.15, it is possible to qualitatively exploit the hybridization model.[27] In fact, Nordlander and co-workers analyse the plasmon coupling of a dimer whose dipoles are oriented parallel or orthogonally to the inter-axes between the nanoparticles (10 nm radius). In Fig. 2 of this article, the authors show how the plasmon energies of both dimer orientations vary as a function of the nanoparticles interdistance. In particular, when dipoles oriented parallel to the dimer axes are considered, two hybridized configurations are possible (bright and dark modes). As the inter-distance decreases, the bonding and anti-bonding dimer plasmons begin to split asymmetrically. The bright and dark modes respectively shift downward and upward in energy, with a quite limited upward shift of the dark mode. The overall effect is a shift to lower energy corresponding to a red-shift of the plasmon resonance wavelength). This effect is more pronounced when the nanoparticles inter-distance is smaller because multipolar effects, responsible of the deviations from the dipolar model[17,18], become relevant. In our case, with larger nanoparticle sizes and very small interparticle gaps

(nearly touching limit) the effect is particularly evident and corresponds to a steeper distance-decay behaviour.

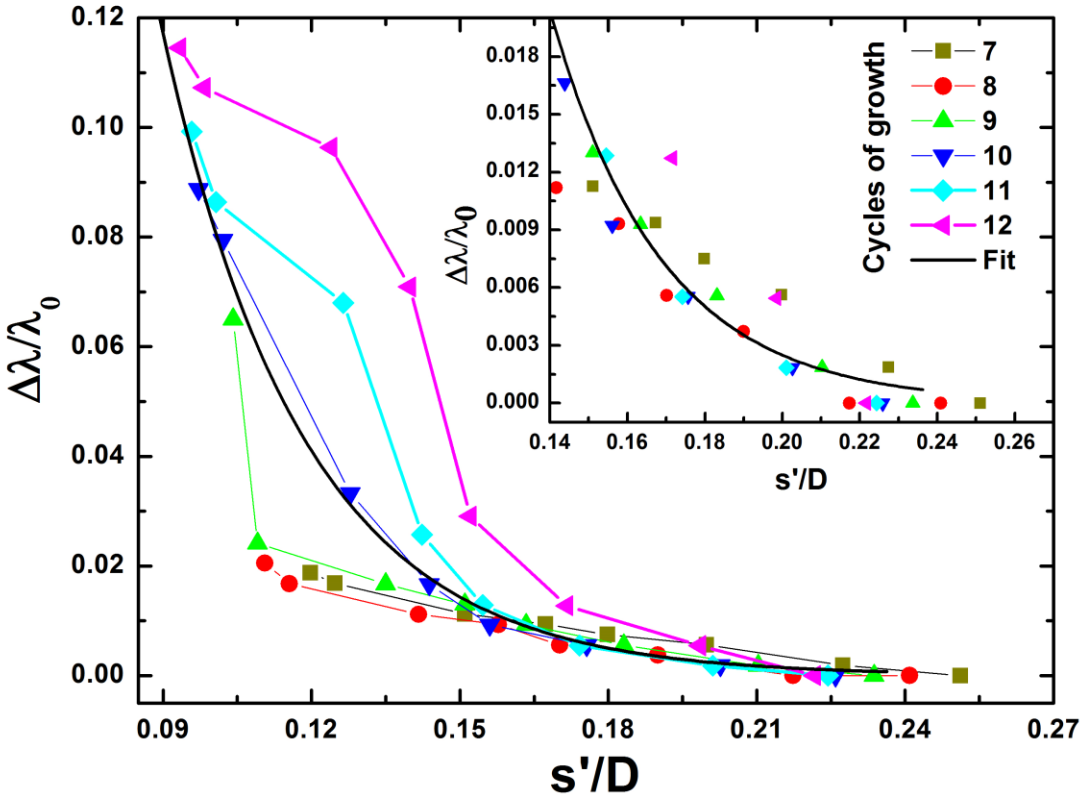

Fig. 4 Experimental dependence of $\Delta\lambda/\lambda_0$ on s'/D (normalized shift and normalized interparticle gap respectively of samples under stretching plotted for samples with a different number of cycles of growth (from seven to twelve cycles). Each absorption spectrum has been acquired while increasing the applied stretching δ (0%; 2.4%; 5.6%; 8.6%; 11.6%; 14.9%; 18.0%; 20.8%).

As a matter of fact, the proposed experimental analysis can be considered as an empirical evidence of the limit of validity of the dipolar model and, at the same time, it represents an opportunity to check the validity of other models (hybridization model) in the nearly touching limit of nanostructures. The aim of a further study will be the quantitative determination of those

experimental conditions that mark the border between a dipolar and a multipolar hybridization description of the plasmon coupling and the exploration of the small gap region (s'/D<0.15) that actually represents the experimental challenge in this kind of research. Instrumental to this aim is the high sensitivity that can be achieved by exploiting the synergy between particle size control (growth process) and the continuous tuning of the interparticle gap (mechanical strain).

Conclusions

We have realized a macroscopic strain-dependent optical pad based on bottom-up, self-assembly principles. Upon a slight stretching, the amorphous and initially isotropic structure reversibly develops a strong polarization-dependent variation of its optical properties, which is accompanied by a macroscopic change of colour. This effect is due to nanoscale changes in inter-particle separations, which have dramatic effects on the plamonic coupling strength between particles. Key for the preparation of the optical pad is the growth of the nanoparticles after their immobilization on the PDMS surface, which reduces the gap between neighbouring particles such that plasmon coupling starts to be effective. The stretching of the PDMS pad then leads to further reduction of the gap between nanoparticles in the direction perpendicular to the stretching which triggers the plasmon coupling. For largely grown particles and large strain the shift of the plasmon resonance reveals multipolar coupling with a clear deviation from the plasmon ruler equation. The possibility of continuously tuning the coupling by applying a macroscopic mechanical solicitation represents the key feature of this novel platform: its exploitation can enable the fundamental study of the plasmon coupling effect, with an

unprecedented sensitivity as well as the realization of advanced applications in sensing and strain detectors.

Experimental

Sample fabrication. Samples have been fabricated in multiple steps. First the PDMS elastomeric template was obtained by mixing in a baker elastomeric and curing agent in 1:10 weight ratio. The mixture was then poured in a glass petri dish. Afterwards, the petri dish was baked in the oven at 80°C for one hour. After the baking step, the hardened PDMS substrate was peeled off from the petri dish and cut into pieces with size of (26 mm x 16.6 mm x 1.2 mm).

Gold nanoparticles (GNPs) synthesis: Milli Q-water (18.2 MΩ-cm); hydrogen tetrachloroaurate (III) ($HAuCl_4$) was purchased from Alfa Aesar; sodium citrate tribasic dehydrate was purchased from Sigma-Aldrich. GNPs were prepared in Milli Q-water according to the well-known Turkevich method:[28] 500 mL of a 0.25 mM solution of $HAuCl_4$ in a vessel under constant magnetic stirring was heated to 100°C in an oil bath. When the solution started boiling, 12.5 mL of 0.03 M sodium citrate was added. During the 15 min of reaction, the solution changed colour (from black to red wine). At the end, the reaction vessel was removed from the oil bath and was left to cool down to room temperature.

To prepare the monolayer of GNPs, used as seeds, the PDMS template was first rinsed with water and ethanol and then dried under a stream of air. Then it was exposed to a plasma (806 mTorr with a constant flux of air of 31.94 mL/min, 90 sec, 7.2 Watt), which leads to the oxidation of the surface. Immediately after this step, the template was dipped in a solution of Milli Q-water and 1% of 3-aminopropyltriethoxysilane (from Sigma Aldrich) for 30 min. The

template was then copiously rinsed with Milli Q-water and dried with a stream of air. At this point, the functionalized template was dipped in GNPs solution for 2.30 hours. After removal from the GNPs solution, the sample was rinsed and dried as described before.

The growing processes of GNPs seeds[29-32] attached on PDMS was realized by dipping the sample in Au^{3+}/NH_2OH solution (0.3 mM $HAuCl_4$, Alfa Aesar), 0.4 mM NH_2OH (Sigma-Aldrich) at room temperature. Each growing cycle lasted 2 minutes. After each step the sample was washed and dried.

Stretching apparatus and acquisition of extinction spectra. For the acquisition of spectra at rest and under stress, a platform was built with two mobile clamps controlled and moved apart by two-micrometer screws. The fabricated platform was positioned in the Varian V-670 UV/VIS/NIR spectrophotometer used for all extinction spectroscopy experiments. The sample was mounted between tweezers (Figs. 1b,c) and positioned perpendicularly to the probe beam. For every step of stretching (relaxing), the corresponding spectrum was acquired. Measurements were acquired both with un-polarized and polarized light. For polarized light experiments, two polarizers were mounted in both the reference and the sample beam paths within the spectrophotometer. In order to obtain the extinction exclusively due to coupled nanoparticles, (excluding any contribution from the flexible substrate) PDMS samples identical to the ones used for the experiments (same size and thickness), but without nanoparticles, were analysed under identical stretching conditions. The extinction spectra of the PDMS substrates have then been subtracted from the spectra of the samples with nanoparticles. This procedure has been repeated for all the analysed samples.

A crosscheck of the operation in elastic regime during all performed experiments was required to guarantee the reliability of obtained results. For this reason, at each stretching state, a picture of the sample was taken and analyzed (with the ImageJ software) to measure the actual length and width of the sample. The obtained values have been used to calculate the percentage compression that the sample undergoes in the direction perpendicular to the applied strain. Within the experimental error, all obtained values up to a stretching percentage of 20.8% (Fig. S1 in Supplementary Information) confirm a Poisson coefficient of about 0.5 (0,4996±0,0283).

Calculation of $\Delta\lambda_\iota/\lambda_0$ and s_i'/D_i values for extinction experiments performed on samples whose nanoparticles have undergone i growth cycles

The absorption spectrum of the sample whose nanoparticles have undergone *i* cycles of growth (*i*=0…12) has been acquired several times by changing, each time, the value of the applied mechanical stress δ (0%; 2.4%; 5.6%; 8.6%; 11.6%; 14.9%; 18.0%; 20.8%). For each δ value, the resonance peak wavelength λ_I was utilized to calculate the plasmon shift normalized to the single-particle resonance wavelength λ_0, $\Delta\lambda_\iota/\lambda_0=(\lambda_\iota-\lambda_0)/\lambda_0$. For what concerns the values assumed by the normalized interparticle gap s_i'/D_i under different stretching conditions, the average diameter D_i has been calculated by assuming an exponential growth of the particles from the initial D_0=23nm (nanoparticles not grown) through D_7=31.1nm (seven growing steps) and up to D_{12}=32nm (twelve growing cycles) as suggested by the fit reported in Fig. S6 (Supplementary Information). We furthermore checked the sensitivity of the results towards the model of growth (exponential vs. linear). In the same Fig. S6, the linear fit between the 7th and the12th cycle of growth is reported, and in Fig. S5 the result of the analysis assuming linear growth is shown. The

comparison between the graph in Fig. S5 and the one reported in Fig. 4 shows that the deviation between the two analyses is negligible.

The average D_0, D_7 and D_{12} values have been calculated by a MatLab script, which analysed the SEM images of the corresponding samples; in particular, images were binarized and, as a result, coordinates and diameters of separated particles were determined (Fig. S4 in Supplementary Information). Subsequently, a K nearest neighbours algorithm was applied to calculate distances (and angles between) the closest particles. This analysis yields a nearest neighbour (center-to-center) separation of r=39 nm (arithmetic average). In presence of stretching and by assuming an elastic elongation of the sample (and a consequent compression in the perpendicular direction), the average interparticle distance can calculated by using the formula $r'=r[(1+\delta)^2\cos^2\alpha+(1-0.5\delta)^2\sin^2\alpha]^{1/2}$. Moreover, results reported in Figs. S8 a,c (Supplementary Information) indicate that, during a stretching experiment while illuminating the sample with ⊥-polarized light, a red-shift of the plasmonic resonance wavelength occurs. Responsible of this shift is the plasmonic coupling effect that is preferentially due to dimers with high values of the angle α ($60°<\alpha<90°$) (see Fig. S8 c). As such, we can assume:

$$\frac{s_i'}{D_i} = \frac{r' - D_i}{D_i} = \frac{r\left[(1+\delta)^2\cos^2\alpha + (1-0.5\delta)^2\sin^2\alpha\right]^{1/2} - D_i}{D_i} \cong \frac{r(1-0.5\delta) - D_i}{D_i} \qquad (5)$$

where the factor 0.5 represents the Poisson's coefficient of the PDMS substrate.

Acknowledgement

The present communication is co-funded by the European Commission, European Social Fund and Calabria Region. Authors are the only responsible of this communication and the European

Commission and Calabria region decline every responsibility on the use that will be done with the contained information. Financial support from the University of Geneva is kindly acknowledged.

References

1 U. Kreibig and M. Vollmer, *Optical properties of metal clusters*, Springer, Berlin, 1995.

2 G. Mie, *Ann. Phys.*, 1908, **25**, 377.

3 S. A. Maier, *Plasmonics: Fundamentals and Applications*, Springer, New York, 2007.

4 N. J. Halas, S. Lal, W. S. Chang, S. Link and P. Nordlander, *Chem. Rev.*, 2011, **111**, 3913.

5 K. H. Su, Q. H. Wei, X. Zhang, J. J. Mock, D. R. Smith and S. Schultz, *Nano Lett.*, 2003, **3**, 1087.

6 K. A. Willets and R. P. Van Duyne, *Ann. Rev. of Phys. Chem.*, 2007, **58**, 267.

7 A. J. Haes, S. L. Zou, G. C. Schatz and R. P. Van Duyne, *J. Phys. Chem. B*, 2004, **108**, 109.

8 J. F. Li, Y. F. Huang, Y. Ding, Z. L. Yang, S. B. Li, X. S. Zhou, F. R. Fan, W. Zhang, Z. Y. Zhou, D. Y. Wu, B. Ren, Z. L. Wang and Z. Q. Tian, *Nature*, 2010, **464**, 392.

9 N. Liu, M. L. Tang, M. Hentschel, H. Giessen and A. P. Alivisatos, *Nature Mater.*, 2011, **10**, 631.

10 J. A. Schuller, E. S. Barnard, W. S. Cai, Y. C. Jun, J. S. White and M. L. Brongersma, *Nature Mater.*, 2010, **9**, 193.

11 C. Rockstuhl, F. Lederer, C. Etrich, T. Pertsch and T. Scharf, *Phys. Rev. Lett.*, 2007, **99**, 017401.

12 E. Bailo and V. Deckert, *Chem. Soc. Rev.*, 2008, **37**, 921.

13 S. K. Ghosh and T. Pal, *Chem. Rev.*, 2007, **107**, 4797.

14 K. M. Mayer and J. H. Hafner, *Chem. Rev.*, 2011, **111**, 3828.

15 M. K. Kinnan and G. Chumanov, *J. Phys. Chem. C*, 2010, **114**, 7496.

16 A. Cunningham, S. Muhlig, C. Rockstuhl and T. Burgi, *J. Phys. Chem. C*, 2011, **115**, 8955.

17 P. K. Jain and M. A. El-Sayed, *Chem. Phys. Lett.*, 2010, **487**, 153.

18 P. K. Jain, W. Y. Huang and M. A. El-Sayed, *Nano Lett.*, 2007, **7**, 2080.

19 C. Sonnichsen, B. M. Reinhard, J. Liphardt and A. P. Alivisatos, *Nature Biotech.*, 2005, **23**, 741.

20 M. G. Millyard, F. M. Huang, R. White, E. Spigone, J. Kivioja and J. J. Baumberg, *Appl. Phys. Lett.*, 2012, **100**, 073101.

21 X. L. Zhu, L. Shi, X. H. Liu, J. Zi and Z. L. Wang, *Nano Res.*, 2010, **3**, 807.

22 X. L. Zhu, S. S. Xiao, L. Shi, X. H. Liu, J. Zi, O. Hansen and N. A. Mortensen, *Opt. Exp.*, 2012, **20**, 5237.

23 Y. L. Chiang, C. W. Chen, C. H. Wang, C. Y. Hsieh, Y. T. Chen, H. Y. Shih and Y. F. Chen, *Applied Physics Letters*, 2010, **96**, 041904.

24 S. Malynych and G. Chumanov, *J. Am. Chem. Soc.*, 2003, **125**, 2896.

25 R. H. Pritchard, P. Lava, D. Debruyne and E. M. Terentjev, *Soft Matter*, 2013, **9**, 6037.

26 M. Kasha, *Radiation Res.*, 1963, **20**, 55M. Kasha, *Radiation Res.*, 1963, **20**, 55.

27 P. Nordlander, C. Oubre, E. Prodan, K. Li, M.I. Stockman, Nano Lett. 2004, **4**, 899−903

28 J. Kimling, M. Maier, B. Okenve, V. Kotaidis, H. Ballot and A. Plech, *J. Phys. Chem. B*, 2006, **110**, 15700.

29 K. R. Brown, L. A. Lyon, A. P. Fox, B. D. Reiss and M. J. Natan, *Chem. Mater.*, 2000, **12**, 314.

30 K. R. Brown and M. J. Natan, *Langmuir*, 1998, **14**, 726.

31 K. R. Brown, D. G. Walter and M. J. Natan, *Chem. Mater.*, 2000, **12**, 306.

32 D. Enders, T. Nagao, A. Pucci, T. Nakayama and M. Aono, *Phys. Chem. Chem. Phys.*, 2011, **13**, 4935.

TOC Figure

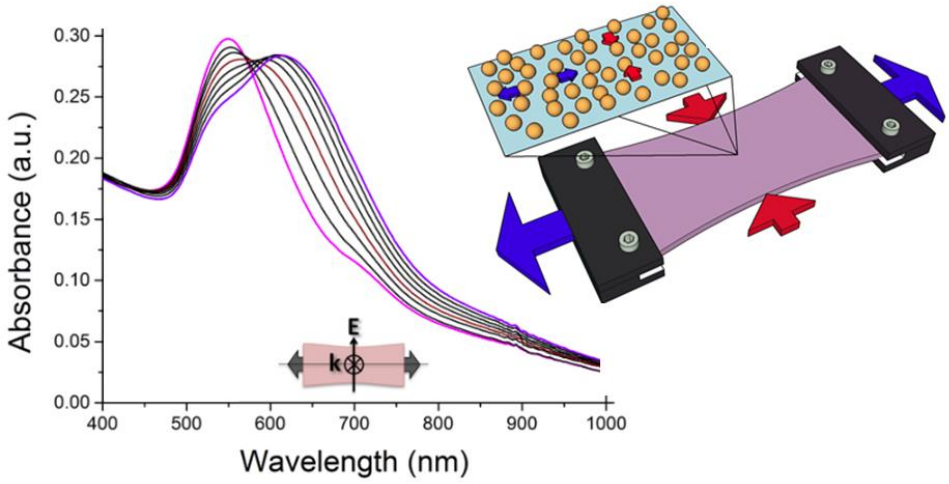

A macroscopic mechanical strain can be used to control the coupling and therefore the electromagnetic field at the nanoscale.